

Heat Exchange Effectiveness Estimation Model for Thermoelectric Cooling and Heating Unit

H. S. Lim, S. Y. Li, W. J. Kim, B. J. Kim and J. W. Jeong

*Department of Architectural Engineering
 Hanyang University, Seoul 04763, Republic of Korea*

SUMMARY

This study proposes an empirical model for predicting the heat exchange effectiveness of a thermoelectric cooling and heating unit. The purpose of a thermoelectric cooling and heating unit is to simultaneously cool and heat liquids using a thermoelectric module and two heat exchangers. Using a mock-up model, 77 experiments were carried out based on six operating parameters: inlet temperature of the cold and hot sides, input current, the specific surface area of heat exchange, and water flow rate through the cold and hot sides. Using the response surface methodology (RSM), collected data was analyzed to develop the prediction models. We considered the design parameters to be non-dimensional factors, therefore the number of transfer units (NTU), inlet temperature, and surface temperature of the cold and hot sides were calculated from the measured operating parameters. As a result, two empirical models predicting the heat exchange effectiveness of cooling and heating were proposed with R^2 values of 0.95 and 0.88, respectively.

INTRODUCTION

In recent years, there has been interest in using thermoelectric modules (TEM) as solid-state non-vapor compression heat pumps (Goetzler et al. 2016) because of the advantages of compact size, simple control, no refrigerant, noiseless operation, higher reliability without moving parts, and a longer lifetime than electric compressors (Al-Nimr Ma et al. 2015; Ramousse et al. 2015).

TEM have also been used for heating, ventilation, and air conditioning in buildings for several years. Irshad et al. (Irshad et al. 2017) proposed a thermoelectric air duct system integrated with photovoltaic wall for space cooling. The optimum design of the proposed system was conducted based on the experiment and simulation in terms of temperature difference between hot and cold sides of the TEM and its cooling capacity. Allouhi et al. (Allouhi et al. 2017) evaluated the thermoelectric heating system used for office room. The heat was reclaimed from the exhaust air at the cold side of TEM and released heat at the hot side of TEM was used for heating the supply air during winter. The suggested system showed 55 to 64 % less energy consumption compared with the conventional electric air heater.

On the other hands, there are few studies using TEM for simultaneous cooling and heating. The performance of air heating and cooling systems using TEM has been investigated in the past through experiments and numerical simulations (Yilmazoglu 2016). The results showed a coefficient of performance of 4.1 for heating and 0.7 for cooling, with the possibility of simultaneous heating and cooling using TEM.

Also, Ramousse and Perier-Muzet (Ramousse and Perier-Muzet 2016) suggested a design for a thermoelectric heat pump based on the minimization of entropy generation method. The proposed system has multi-channel heat exchangers for cooling and heating using working fluids simultaneously. The optimal ratio of heat exchange area for heating and cooling was 4 in the proposed thermoelectric heat pump system. However, no study has evaluated the detailed performance of TEM for cooling and heating at the same time. Accordingly, no prediction models currently exist to estimate the simultaneous heating and cooling performance using TEM.

In this study, a thermoelectric unit for liquid cooling and heating was investigated using a mock-up model. The experimental data of the thermoelectric cooling and heating unit were collected from in-situ operations. Based on the data, the effects individually and interactively of each design parameter on heat exchange effectiveness were also evaluated statistically. An empirical model for predicting heat exchange effectiveness of a thermoelectric cooling and heating unit was developed using the response surface methodology (RSM).

MOCK-UP MODEL

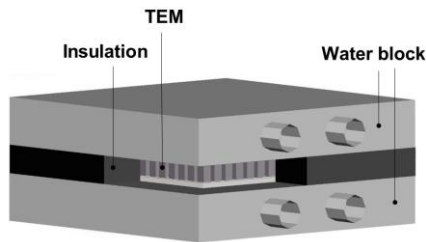
As shown in figure 1 and 2, the TEM is sandwiched between water blocks made of hollow aluminum with high thermal conductivity. The water block is the heat exchanger between a liquid and the constant-temperature surface of the TEM. Teflon insulation was also attached, to prevent heat conduction from the hot side to the cold side. The six thermoelectric cooling and heating units were connected in series, and the water for heating and cooling was supplied through upper and lower pipes by two pumps. All water pipes with 8-mm diameter were insulated using foam-rubber insulation and units were insulated with compressed polystyrene foam.

Two self-priming diaphragm water pumps were used with the range of water flow between 0 to 0.034 kg/s with the maximum head 3 m. The water flow rates of the cold and hot sides could also be controlled independently using a controller.

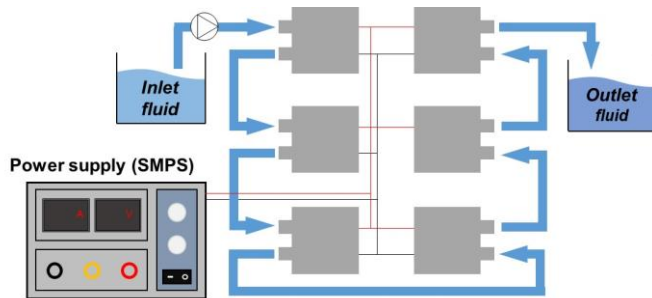
The Technical specifications of TEM is shown in Table 1. When the direct current flows into the TEM, the heat is moved from the cold side to hot side by Peltier effect. In this system, the input current could be controlled up to 30 A and 30 V using the switched mode power supply (SMPS) and the number of units could be changed manually to control the experiments. However, maximum input current and voltage to the TEM were used within 4.2 A and 24.5 V, independently, for preventing the break-down of the TEM.

Table 1. Technical specification of TEM (HMN 6055)

Description	Value
Dimension	55 × 55 × 3.7
I_{max}	5.0 A
V_{max}	28.2 V
Q_{max}	106 W ($T_{hot} = 25\text{ }^{\circ}\text{C}$)
	120 W ($T_{hot} = 50\text{ }^{\circ}\text{C}$)
ΔT_{max}	68 $^{\circ}\text{C}$ ($T_{hot} = 25\text{ }^{\circ}\text{C}$)
	77 $^{\circ}\text{C}$ ($T_{hot} = 50\text{ }^{\circ}\text{C}$)

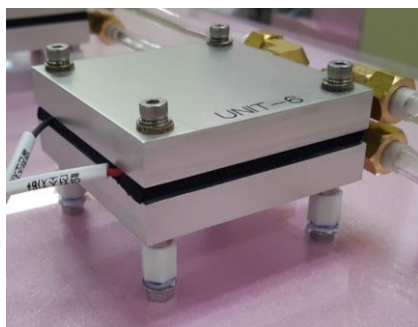


(a) TEM cooling and heating unit

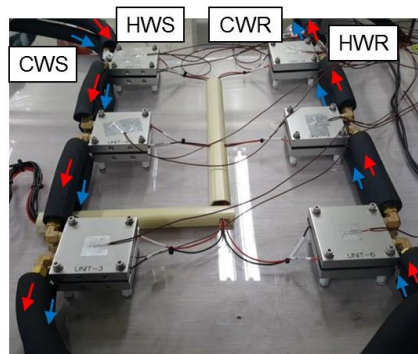


(b) TEM cooling and heating system

Figure 1. Schematic diagram of TEM cooling and heating unit and system.



(a) TEM cooling and heating unit



(b) TEM cooling and heating system

Figure 2. In-situ TEM cooling and heating unit and system.

MEASUREMENT CONFIGURATION

There are six operating parameters: input current (I), inlet temperature of the hot side ($T_{h,in}$), inlet temperature of the cold side ($T_{c,in}$), water flow rate of hot side ($\dot{m}_{h,w}$), water flow rate of cold side ($\dot{m}_{c,w}$), and the specific surface area for heat exchange (A_{hx}). In addition, outlet temperature of the hot side ($T_{h,out}$) and cold side ($T_{c,out}$) were measured. Each water block we used has a heat exchange area of 0.0045 m^2 as shown in figure 3. We used six water blocks, therefore the total heat exchange area was varied from 0.0045 m^2 to 0.027 m^2 . The minimum, maximum and intermediate values for operating parameters are shown in Table 2.

The operating range of each parameter was determined as wide as possible based on the limitations of the equipment used in the experiment. In addition, we considered the intermediate value to account for the possibility of a non-linear prediction model. We used a central composite design (CCD) approach with face centered (Myers et al. 2009) that can be applied on the response surface methodology (RSM) in order to develop the quadratic model deriving the heat exchange effectiveness.

In CCD, the experimental cases were designed in three parts: the 2^k factorial design matrix, the axial point matrix, and the center point matrix. The 2^k factorial design matrix is combinations of minimum and maximum value of each operating parameters, where k is the number of parameters. The axial point matrix is composed of minimum or maximum value of one operating parameter and the intermediate value of the remaining parameters. Thereby, the number of axial point matrix is $2k$. A center point matrix is the intermediate value of all operating parameters. As a results, total 77 experiment sets, that is 64 sets from 2^k factorial design matrix, 12 sets from axial point matrix, and 1 set from the center point matrix, were made.

The input current (I) was modulated using SMPS, and water flow rates (\dot{m}) of both cold and hot sides were controlled by the direct current motor speed controller connected with each pump. The inlet water temperatures of both cold and hot sides were set using the electric water heaters. The heat exchange area was adjusted by changing the number of used TEM units. In the experiments, the temperature were measured using T-type thermocouple with MV 1000 data logger within the range of -200 to $400\text{ }^{\circ}\text{C}$ with $\pm 0.5\text{ }^{\circ}\text{C}$ accuracy. Measurements were performed for ten minutes at one-second interval when the all measurement points showed stable values. The input current and water flow rates were continuously maintained at their set-points in each experiment.

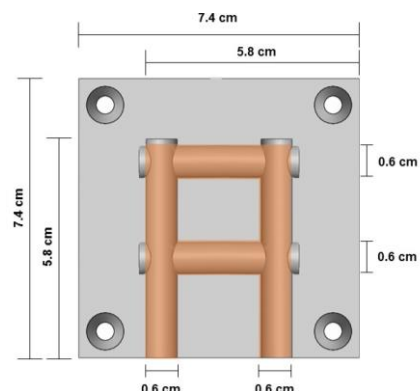


Figure 3. Sectional diagram of the water block.

Table 2. Operating parameters for experiments

Operating parameters	Ranges		
	Min.	Intermediate values	Max.
I [A]	1	2.5	4.2
$T_{h,in}$ [°C]	45	55	65
$T_{c,in}$ [°C]	15	25	35
$\dot{m}_{w,h}$ [kg/s]	0.010	0.014	0.020
$\dot{m}_{w,c}$ [kg/s]	0.010	0.014	0.020
A_{hx} [m ²]	0.005	0.014	0.027

Temperature measurements were conducted using a T-type thermocouple recorded with a MV 1000 data logger. We did not measure the input current and water flow rates because those values were consistently maintained at set points in each experiment.

OPERATING DATA

A total of 57 sets of data from the 77 experiments were used for developing an empirical model for heat exchange effectiveness. Twenty data sets were excluded as outliers due to their temperature difference between inlet and outlet of the hot and cold sides of the water block being too small. A temperature difference lower than the accuracy of the temperature sensor (± 0.5 °C) was regarded meaningless in this study.

These outliers appeared when the TEM cooling and heating unit did not produce the meaningful temperature variation between the inlet and outlet at both hot side and cold side. The negligible water temperature differences between inlet and outlet of the TEM heat pump were observed when the inlet water temperature between hot and cold sides was too large, so the Seebeck effect overrides the Peltier effect.

In the Seebeck effect, the heat is transferred from the hot side to cold side and the TEM generates the electricity. On the other hands, in the Peltier effect, the heat is transferred from the cold side to hot side by supplying electric power from outside, and the TEM works as a heat pump. These two effects are occurred simultaneously, so the Peltier effect should be dominant by supplying the proper magnitude of input current enough to offset the Seebeck effect if one wants to use the TEM units as heat pump; otherwise, the TEM heat pump cannot produce meaningful temperature difference of the water between the inlet and outlet in both hot and cold sides.

Figure 4 shows the data from the representative experiment sets. In the initial stage, surface temperature difference between the cold and hot sides increased rapidly as the outlet water temperature changed. As time went on, the temperatures converged stably. In this representative case, the inlet temperature difference of water was 10°C and the outlet temperature difference of water was 30°C. Therefore, the possibility of simultaneous cooling and heating using TEM was verified based on the mock-up experiments. Using equations (1) and (2), the heat exchange effectiveness were calculated as 0.828 for cooling and 0.809 for heating in average.

$$\varepsilon_c = \frac{T_{c,in} - T_{c,out}}{T_{c,in} - T_{c,surf}} \quad (1)$$

$$\varepsilon_h = \frac{T_{h,out} - T_{h,in}}{T_{h,surf} - T_{h,in}} \quad (2)$$

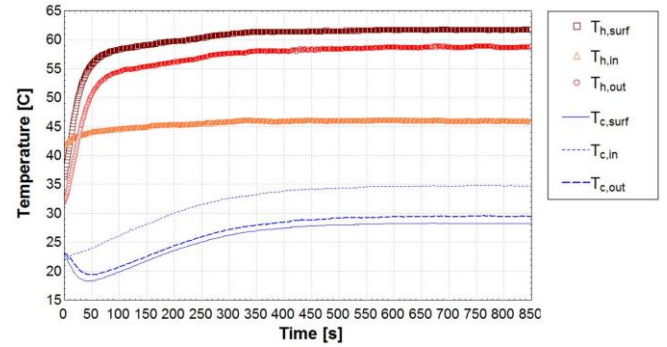


Figure 4. Thermal behavior in thermoelectric cooling and heating unit in the representative experimental case.

DESIGN PARAMETERS

The experiments were conducted using six measurement parameters. However, the model development was based on the following six design parameters: number of transfer units for cooling and heating (NTU_c and NTU_h), inlet temperature of the cold and hot sides ($T_{c,in}$ and $T_{h,in}$), and surface temperature of the cold and hot sides ($T_{c,surf}$ and $T_{h,surf}$). The measurement parameters and design parameters were different, in order to develop a non-dimensional model. In addition, the dependent variables were not the directly-measured outlet temperature of the cold and hot sides ($T_{c,out}$ and $T_{h,out}$). Instead, they were the calculated heat exchange effectiveness for cooling and heating (ε_c and ε_h) using equations (1) and (2).

In previous studies, many researchers showed the effectiveness of heat exchangers, generally using the effectiveness–NTU method (Cengel 2007). Similarly, we considered the TEM cooling and heating unit part of the heat exchanger. Therefore, the proposed model can predict the effectiveness of the heat exchanger and the outlet temperature of the cold and hot sides.

The water mass flow rate (\dot{m}_w) and the specific surface area of heat exchange (A_{hx}) were limited in the mock-up model used in this study. Moreover, the water had its own properties such as specific heat (c_p), density (ρ), viscosity (μ), etc. Therefore, we considered using NTU in order to expand the applicability of the proposed model.

NTU was derived using equation (3) and the convection heat transfer coefficient (h) was calculated using equation (4). In this study, the heat conductivity (κ) of water used was 0.6 W/m·°C and the pipe diameter (d) was 6 mm. The Nusselt number (Nu) was calculated using equation (5) (Gnielinski 1976), which is suitable to be used for turbulent flow in tubes. Using equation (6), the Reynolds number (Re) was calculated between 2,380 and 9,600. The Prandtl number (Pr) was assumed to be constant at 1.75. Using equation (7) (Petukhov 1970), the friction factor (f) can be derived.

$$NTU = \frac{hA_{hx}}{\dot{m}c_p} \quad (3)$$

$$h = \frac{Nu \times \kappa}{d} \quad (4)$$

$$Nu = \frac{(f/8) \times (Re - 1000) \times Pr}{1 + 12.7(f/8)^{0.5} (Pr^{2/3} - 1)} \quad \left(\begin{array}{l} 0.5 \leq Pr \leq 2000 \\ 3 \times 10^3 < Re < 5 \times 10^6 \end{array} \right) \quad (5)$$

$$Re = \frac{\rho V d}{\mu} \quad (6)$$

$$f = (0.79 \times \ln(Re) - 1.64)^{-2} \quad (7)$$

Where ρ is the density of water, V is the velocity of water and μ is the viscosity of water.

The TEM cooling and heating unit in this study is a type of water-to-water heat exchanger if we consider the TEM to be a heat bridge. However, TEM works as a heat pump using the Peltier effect, so heat flows from low temperature to high temperature. The driving force of the Peltier effect is electricity and the input current is an important factor in the TEM cooling and heating unit. Despite this, input current is not included in design parameters because all TEM have different electrical characteristics such as maximum input current and voltage. Instead, we considered the surface temperature of the cold and hot sides. If input current is increased, the temperature difference between the cold and hot sides should also increase. In contrast, temperature difference between both sides should decrease as input current decreases.

MODEL DEVELOPMENT

To develop the empirical model, a statistical analysis was conducted using Design Expert Version 10. The analysis of variance (ANOVA) and response surface methodology (RSM) (Jones 1997) were accomplished based on the operation data sets containing 4,617 samples. As a result, two prediction models for the effectiveness of heat exchange in the TEM cooling and heating unit were developed as a function of the six design parameters. The two-factor interaction model (2FI) and quadratic model were selected as modelling methodology for cooling and heating. The heat exchange effectiveness prediction model for cooling and heating show the R^2 value of 0.947 and 0.883, respectively. An ANOVA statistically validated the significance of model parameters and all the parameters in the models showed high significance with p-value below 0.01 as shown in Table 3.

The proposed models for effectiveness of heat exchange in the TEM cooling and heating unit are shown in equations (8) and (9). The coefficients of each model are described in Table 4. The valid ranges of each design parameter are summarized in Table 5.

$$\begin{aligned} \varepsilon_c = & \alpha_0 + \alpha_1 \times NTU_c + \alpha_2 \times NTU_h + \alpha_3 \times T_{c,in} + \alpha_4 \times T_{h,in} + \\ & \alpha_5 \times T_{c,surf} + \alpha_6 \times T_{h,surf} + \alpha_7 \times NTU_c \times NTU_h + \alpha_8 \times \\ & NTU_c \times T_{c,in} + \alpha_9 \times NTU_c \times T_{h,in} + \alpha_{10} \times NTU_c \times T_{c,surf} + \\ & \alpha_{11} \times NTU_c \times T_{h,surf} + \alpha_{12} \times NTU_h \times T_{c,in} + \alpha_{13} \times NTU_h \times \\ & T_{h,in} + \alpha_{14} \times NTU_h \times T_{c,surf} + \alpha_{15} \times NTU_h \times T_{h,surf} + \alpha_{16} \times \\ & T_{c,in} \times T_{c,surf} + \alpha_{17} \times T_{c,in} \times T_{h,surf} + \alpha_{18} \times T_{h,in} \times T_{c,surf} + \alpha_{19} \times \\ & T_{h,in} \times T_{h,surf} + \alpha_{20} \times T_{c,surf} \times T_{h,surf} \end{aligned} \quad (8)$$

$$\begin{aligned} \varepsilon_h = & \alpha_0 + \alpha_1 \times NTU_c + \alpha_2 \times NTU_h + \alpha_3 \times T_{c,in} + \alpha_4 \times T_{h,in} + \\ & \alpha_5 \times T_{c,surf} + \alpha_6 \times T_{h,surf} + \alpha_7 \times NTU_c \times NTU_h + \alpha_8 \times \\ & NTU_c \times T_{c,in} + \alpha_9 \times NTU_c \times T_{h,in} + \alpha_{10} \times NTU_c \times T_{c,surf} + \\ & \alpha_{11} \times NTU_c \times T_{h,surf} + \alpha_{12} \times NTU_h \times T_{c,in} + \alpha_{13} \times NTU_h \times \\ & T_{h,in} + \alpha_{14} \times NTU_h \times T_{c,surf} + \alpha_{15} \times NTU_h \times T_{h,surf} + \alpha_{16} \times \\ & T_{c,in} \times T_{h,in} + \alpha_{17} \times T_{c,in} \times T_{c,surf} + \alpha_{18} \times T_{c,in} \times T_{h,surf} + \alpha_{19} \times \\ & T_{h,in} \times T_{c,surf} + \alpha_{20} \times T_{h,in} \times T_{h,surf} + \alpha_{21} \times T_{c,surf} \times T_{h,surf} + \end{aligned}$$

$$\alpha_{22} \times NTU_c^2 + \alpha_{23} \times NTU_h^2 + \alpha_{24} \times T_{c,in}^2 + \alpha_{25} \times T_{c,surf}^2 + \alpha_{26} \times T_{h,surf}^2 \quad (9)$$

Table 3. ANOVA results of the heat exchange effectiveness for cooling and heating

(a) Heat exchange effectiveness for cooling

Source	Sum of Squares	df	Mean Square	F	Sig.
Model	334.7	20	16.7	4121	0.00
A: NTU _c	0.1	1	0.1	17	0.00
B: NTU _h	2.2	1	2.2	541	0.00
C: T _{c, in}	1.7	1	1.7	421	0.00
D: T _{h, in}	0.7	1	0.7	162	0.00
E: T _{c, surf}	1.4	1	1.4	343	0.00
F: T _{h, surf}	1.3	1	1.3	310	0.00
AB	4.3	1	4.3	1059	0.00
AC	1.3	1	1.3	308	0.00
AD	1.7	1	1.7	412	0.00
AE	0.4	1	0.4	86	0.00
AF	1.2	1	1.2	300	0.00
BC	1.0	1	1.0	250	0.00
BD	1.4	1	1.4	345	0.00
BE	0.5	1	0.5	125	0.00
BF	1.8	1	1.8	440	0.00
CE	0.1	1	0.1	31	0.00
CF	0.3	1	0.3	68	0.00
DE	2.4	1	2.4	590	0.00
DF	0.5	1	0.5	112	0.00
EF	1.2	1	1.2	294	0.00
Residual	18.7	4595	0.0		
Cor. Total	353.3	4615			

(b) Heat exchange effectiveness for heating

Source	Sum of Squares	df	Mean Square	F	Sig.
Model	65.4	26	2.5	1334	0.00
A: NTU _c	0.0	1	0.0	18	0.00
B: NTU _h	0.0	1	0.0	15	0.00
C: T _{c, in}	0.3	1	0.3	152	0.00
D: T _{h, in}	9.8	1	9.8	5194	0.00
E: T _{c, surf}	0.8	1	0.8	398	0.00
F: T _{h, surf}	6.5	1	6.5	3424	0.00
AB	0.1	1	0.1	42	0.00
AC	0.5	1	0.5	271	0.00
AD	0.3	1	0.3	157	0.00
AE	0.5	1	0.5	284	0.00
AF	0.3	1	0.3	150	0.00
BC	0.4	1	0.4	217	0.00
BD	1.2	1	1.2	617	0.00
BE	0.4	1	0.4	211	0.00
BF	0.9	1	0.9	466	0.00
CD	0.3	1	0.3	166	0.00
CE	0.1	1	0.1	26	0.00
CF	0.2	1	0.2	108	0.00
DE	0.2	1	0.2	129	0.00
DF	0.2	1	0.2	107	0.00
A ²	0.2	1	0.2	83	0.00
B ²	0.0	1	0.0	19	0.00
C ²	0.1	1	0.1	59	0.00
E ²	0.1	1	0.1	47	0.00
F ²	0.0	1	0.0	12	0.00
Residual	8.7	4589	0.00		
Cor. Total	74.1	4615			

Table 4. Coefficients of proposed models

(a) Heat exchange effectiveness for cooling

α_0	α_1	α_2	α_3	α_4	α_5
1.324	2.132	-0.220	-0.078	-0.102	0.149
α_6	α_7	α_8	α_9	α_{10}	α_{11}
0.025	1.542	-0.210	-0.157	0.142	0.115
α_{12}	α_{13}	α_{14}	α_{15}	α_{16}	α_{17}
0.151	0.089	-0.127	-0.091	-0.001	0.002
α_{18}	α_{19}	α_{20}			
0.003	0.001	-0.004			

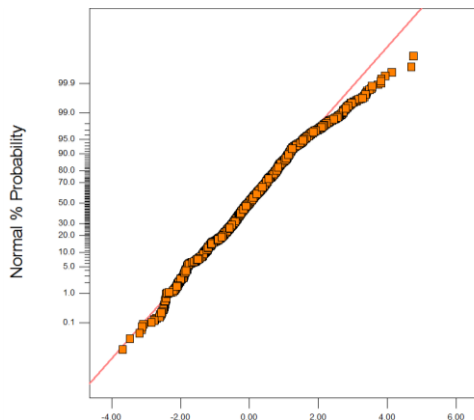
(b) Heat exchange effectiveness for heating

α_0	α_1	α_2	α_3	α_4	α_5
1.368	-2.022	1.022	0.129	-0.024	-0.110
α_6	α_7	α_8	α_9	α_{10}	α_{11}
-0.023	2.423	0.349	0.085	-0.318	-0.084
α_{12}	α_{13}	α_{14}	α_{15}	α_{16}	α_{17}
-0.190	-0.105	0.177	0.103	-0.007	0.009
α_{18}	α_{19}	α_{20}	α_{21}	α_{22}	α_{23}
0.005	0.006	0.001	-0.005	-1.765	-0.981
α_{24}	α_{25}	α_{26}			
-0.006	-0.003	-0.001			

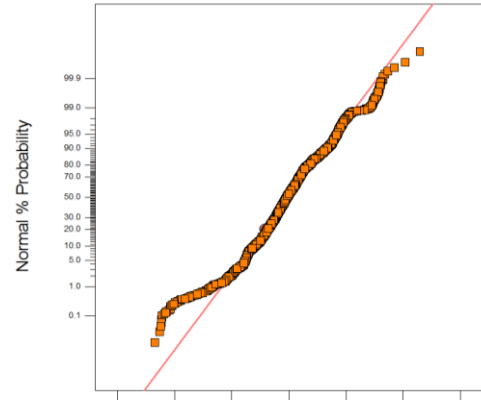
Table 5. The valid range of the proposed models

Operation parameter	Low	High
NTU _c	0.09	0.91
NTU _h	0.19	1.50
T _{c, in}	15.4	37.6
T _{h, in}	42.1	65.4
T _{c, surf}	12.3	34.0
T _{h, surf}	44.9	76.6

As shown in figure 5, a normalized probability plot of the proposed models showed agreement with the normal distribution line. In addition, the predicted heat exchange effectiveness for cooling and heating using proposed models were compared with the actual values in figure 6. Both prediction models of heat exchange effectiveness for cooling and heating were consistent with high R² values of 0.947 for cooling side and 0.883 for heating side.

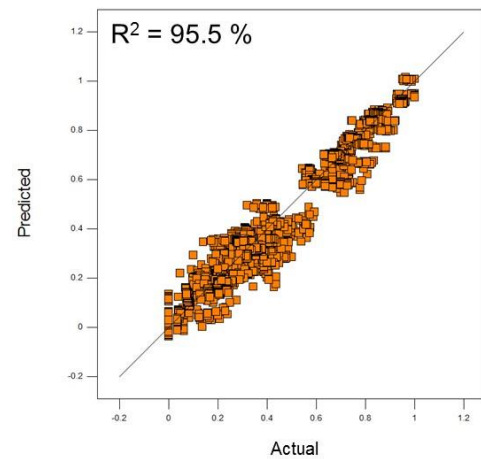


(a) Heat exchange effectiveness for cooling

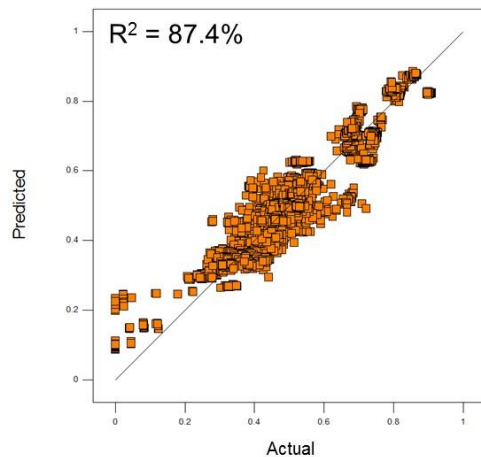


(b) Heat exchange effectiveness for heating

Figure 5. Normal plot of residuals for each proposed model



(a) Heat exchange effectiveness for cooling



(b) Heat exchange effectiveness for heating

Figure 6. Comparison of predicted and actual heat exchange effectiveness for cooling and heating

CONCLUSIONS

The purpose of this study was to estimate performance of a thermoelectric cooling and heating unit when it is used for cooling and heating at the same time. In addition, we developed a prediction model of the heat exchange effectiveness for cooling and heating. Using a mock-up experimental model of a thermoelectric cooling and heating unit, 57 sets of experimental data were collected. The

proposed model was developed using RSM. Six dimensionless design parameters were derived as major factors that should be considered in the design of a thermoelectric cooling and heating unit. The effects of each design parameter on the heat exchange effectiveness were also evaluated using ANOVA. Design parameters and their interactions showed significant effects on the heat exchange effectiveness in both models for cooling and heating. Consequently, prediction models for heat exchange effectiveness were derived with R^2 values of 94.7% and 88.3% for cooling and heating, respectively.

The proposed models can be used for finding optimal operation conditions of a thermoelectric cooling and heating unit. Although the proposed models have a limitation in valid operation ranges, they can be used with various water block-type heat exchangers and TEMs. In addition, we expect this model can be utilized to design a new application of a thermoelectric cooling and heating unit for heating ventilation and air conditioning (HVAC) systems.

ACKNOWLEDGEMENT

This work was supported by a National Research Foundation (NRF) of Korea (No. 2015R1A2A1A05001726), the Korea Agency for Infrastructure Technology Advancement (KAIA) grant (17CTAP-C116268-02), and the Korea Institute of Energy Technology Evaluation and Planning (KETEP) (No. 20164010200860).

REFERENCES

Allouhi A. Boharb A. Ratlamwala T. Kousksou T. Amine M.B. Jamil A. Msaad A.A. 2017. Dynamic analysis of a thermoelectric heating system for space heating in a continuous-occupancy office room, *Appl. Therm. Eng.*, Vol. 113, pp. 150–159

Al-Nimr MA. Tashtoush BM. Jaradat AA. 2015. Modeling and simulation of thermoelectric device working as a heat pump and an electric generator under Mediterranean climate, *Energy*, Vol. 90, pp.1239–50

Cengel Y.A. 2007. *Heat and Mass Transfer: A Practical Approach*, 3rd ed., Boston: McGraw-Hill, New York

Gnielinski V. 1976. *New Equations for Heat and Mass Transfer in Turbulent Pipe and Channel Flow*, *Int. Chem. Eng.*, Vol. 16

Goetzler W. Guernsey M. Young J. Fuhrman J. Abdelaziz O. 2016. *The Future of Air Conditioning for Buildings*, U. S. Department of energy

Irshad K. Habib K. Basrawi F. Saha B.B. 2017. Study of a thermoelectric air duct system assisted by photovoltaic wall for space cooling in tropical climate, *Energy*, Vol. 119, pp. 504–522

Jones R. 1997. *Design and Analysis of Experiments* (fifth edition), John Wiley & Sons, Inc, Publication

Myers R. H. Montgomery D. C. Anderson-cook C. M. 2009. *Response surface methodology*, John Wiley & Sons, Inc, Publication

Peltier Technology Co., Ltd. 2016. *Technical Data Sheet for HMN6055*

Petukhov B.S. 1970. *Heat Transfer and Friction in Turbulent Pipe Flow with Variable Physical Properties*, *Adv. Heat Transf.*, Vol. 6, pp. 503–564

Ramousse J. Perier-Muzet M. 2016. Entropy generation minimization in thermoelectric heat pump systems with multi-channel heat exchangers, *Int J Thermodyn.*, Vol. 19, pp. 82–90.

Ramousse J. Sgorlon D. Fraisse G. Perier-Muzet M. 2015. Analytical optimal design of thermoelectric heat pumps, *Appl. Therm. Eng.*, Vol. 82, pp. 48–56

Yilmazoglu M. Z. 2016. Experimental and numerical investigation of a prototype thermoelectric heating and cooling unit, *Energy Build.*, Vol. 113, pp. 51